# Chemical Vapor Deposition of TiN from Tetrakis(dimethylamido)titanium and Ammonia: Kinetics and Mechanistic Studies of the Gas-Phase Chemistry

**Bruce H. Weiller**

*Contribution from The Aerospace Corporation, Mechanics and Materials Technology Center, P.O. Box 92957/M5-753, Los Angeles, California 90009-2957*

*Received October 16, 1995. Revised Manuscript Received April 3, 1996*[⊗]

**Abstract:** The gas-phase kinetics of the reaction of tetrakis(dimethylamido)titanium ($Ti(NMe_2)_4$) with $NH_3$ have been measured using a flow tube reactor and FTIR spectrometer. $Ti(NMe_2)_4$ reacts rapidly with $NH_3$ in a transamination reaction to form $HNMe_2$ as a direct product. The bimolecular rate constant for the reaction of $Ti(NMe_2)_4$ with $NH_3$ at 24 °C is $k = (1.2 \pm 0.2) \times 10^{-16}$ cm$^3$ molecules$^{-1}$ s$^{-1}$. A primary kinetic isotope effect of $k_H/k_D = 2.6 \pm 0.4$ is observed with $ND_3$ indicating that cleavage of an N−H bond is the rate limiting step. Therefore the rate constant is assigned to the initial transamination reaction with $NH_3$. The temperature dependence of the rate constant gives activation parameters of $\log(A) = -10.0 \pm 0.2$ ($\Delta S^{\dagger} = -19$ cal/(mol K)) and $E_a = 8.1 \pm 0.1$ kcal/mol ($\Delta H^{\dagger} = 6.9 \pm 0.1$ kcal/mol). When excess $HNMe_2$ is added to the gas flow, the reaction rate is strongly suppressed. This is evidence for a reversible initial transamination reaction: $Ti(NMe_2)_4 + NH_3 \rightleftarrows (Me_2N)_3Ti{-}NH_2 + HNMe_2$. The proposed mechanism for subsequent reaction is elimination of $HNMe_2$: $(Me_2N)_3Ti{-}NH_2 \rightarrow (Me_2N)_2Ti{=}NH + HNMe_2$. From the dependence of the observed rate constant on $HNMe_2$, the branching ratio is obtained for the above elimination reaction versus reaction with $HNMe_2$: $(Me_2N)_3Ti{-}NH_2 + HNMe_2 \rightarrow Ti(NMe_2)_4 + NH_3$. The relevance of these results to the chemical vapor deposition of TiN by this chemistry is discussed.

## Introduction

Titanium nitride (TiN) has many useful properties including high hardness, good electrical conductivity, high melting point, and chemical inertness.[1] The applications have included wear-resistant coatings on machine tools and bearings, thermal control coatings for windows,[2] and erosion resistant coatings for spacecraft plasma probes.[3] However, an important new application of TiN is as a diffusion barrier layer for metalization in integrated circuits.

In the fabrication of integrated circuits, electrical contacts are formed at interfaces between metal and semiconductor layers. These interfaces are often not stable due to the diffusion of the metal into the semiconductor and can lead to device failure. A common solution to this problem is a diffusion barrier, a thin sandwich layer that is electrically conductive and blocks diffusion of the metal. TiN is one of the best diffusion barrier materials for silicon integrated circuits due to slow diffusion rates and good electrical conductivity.[4]

Future generations of integrated circuits will require much higher integration densities with feature sizes of less than 350 nm.[5] In order to achieve these goals, highly conformal coatings of TiN are needed on the high-aspect-ratio nanostructures found in integrated circuits. Although TiN is easily deposited by sputtering, this line-of-site technique cannot provide the step coverage required.[6] Chemical vapor deposition (CVD) is superior in this regard but the temperature used to deposit TiN must be below ∼350 °C to be compatible with mutilevel metalization schemes.

Two paths have been demonstrated for the CVD of TiN for microelectronics: (a) titanium tetrachloride ($TiCl_4$) and ammonia ($NH_3$)[2] and (b) tetrakis(dialkylamido)titanium ($Ti(NR_2)_4$) and $NH_3$.[7] Although the chloride reaction gives excellent step coverage,[8] the temperature requirement is too high for this application and Cl contamination is a problem as well. The step coverage is not as good from the amido reaction but it gives TiN at the required temperature. Therefore, improving the step coverage of this process is highly desirable and there has been much recent effort toward this goal.[9−12]

CVD is a complex chemical process in which both gas-phase and surface reactions play a role. It has been shown that gas-phase chemistry is particularly important in this system. When

[⊗] Abstract published in *Advance ACS Abstracts,* May 1, 1996.

(1) Toth, L. E. Refractory Materials; Academic Press: New York, 1971; Vol. 7, Transition Metal Carbides and Nitrides.

(2) Kurtz, S. R.; Gordon, R. G. *Thin Solid Films* **1986**, *140*, 277−290 and references therein.

(3) (a) Wahlstrom, M. K.; Johansson, E.; Veszelei, E.; Bennich, P.; Olsson, M.; Hogmark, S. *Thin Solid Films* **1992**, *220*, 315−320. (b) Veszelei, M.; Veszelei, E. *Thin Solid Films* **1993**, *236*, 46−50.

(4) (a) Wittmer, M.; Melchor, H. *Thin Solid Films* **1982**, *93*, 397−405. (b) Nowicki, R. S.; Nicolet, M. A. *Thin Solid Films* **1982**, *96*, 317−326.

(5) *Solid State Technol.* **1995**, *38 (2)*, 42−50.

(6) The term step coverage is used to describe the conformality of a coating over surface microstructures such as steps, trenches, or vias.

(7) (a) Fix, R. M.; Gordon, R. G.; Hoffman, D. M. *Mater. Res. Soc. Symp. Proc.* **1990**, *168*, 357−362. (b) Fix, R. M.; Gordon, R. G.; Hoffman, D. M. *J. Am. Chem. Soc.* **1990**, *112*, 7833−7835. (c) Fix, R. M.; Gordon, R. G.; Hoffman, D. M. *Chem. Mater.* **1991**, *3*, 1138−1148.

(8) Yokoyama, N.; Hinode, K.; Homma, Y. *J. Electrochem. Soc.* **1991**, *138*, 190−195.

(9) (a) Ishihara, K.; Yamazaki, K.; Hamada, H.; Kamisako, K.; Tarui, Y. *Jpn. J. Appl. Phys.* **1990**, *29*, 2103−2105. (b) Sandhu, G. S.; Meikle, S. G.; Doan, T. T. *Appl. Phys. Lett.* **1993**, *62*, 240. (c) Intemann, A.; Koerner, H.; Koch, F. *J. Electrochem. Soc.* **1993**, *140*, 3215−3222.

(10) (a) Katz, A.; Feingold, A.; Nakahara, S.; Pearton, S. J.; Lane, E.; Geva, M.; Stevie, F. A.; Jones, K. *J. Appl. Phys.* **1992**, *71*, 993−1000. (b) Sun, S. C.; Tsai, M. H. *Thin Solid Films* **1994**, *253*, 440−444.

(11) (a) Dubois, L. H.; Zegarski, B. R.; Girolami, G. S. *J. Electrochem. Soc.* **1992**, *139*, 3603−3609. (b) Prybyla, J. A.; Chiang, C.-M.; Dubois, L. H. *J. Electrochem. Soc.* **1993**, *140*, 2695. (c) Dubois, L. H. *Polyhedron* **1994**, *13*, 1329−1336.

(12) (a) Raaijmakers, I. J.; Vrtis, R. N.; Yang, J.; Ramaswami, S.; Lagendijk, A.; Roberts, D. A.; Broadbent, E. K. *Mater. Res. Soc. Symp. Proc.* **1992**, *260*, 99−105. (b) Raijmakers, I. J. *Thin Solid Films* **1994**, *247*, 85−93. (c) Raaijmakers, I. J.; Yang, J. *Appl. Surf. Sci.* **1993**, *73*, 31−41.

S0002-7863(95)03468-8 CCC: $12.00 

$Ti(NR_2)_4$ is used alone to deposit TiN,[7,13] the resulting material is severely contaminated with carbon. In order to produce low-carbon, low-resistivity TiN from this precursor, reaction with $NH_3$ is required.[7,11] Gas-phase reaction between $Ti(NMe_2)_4$ and $NH_3$ occurs rapidly even at 25 °C to produce $HNMe_2$.[11] This is consistent with studies of the solution chemistry of these compounds that showed transamination reactions between $Ti(NR_2)_4$ and $HNR'_2$ occur readily to form $HNR_2$ and $Ti(NR_2)_{4-n}(NR'_2)_n$ as shown below.[14]

$$Ti(NR_2)_4 + nHNR'_2 \rightarrow Ti(NR_2)_{4-n}(NR'_2)_n + nHNR_2 \qquad (1)$$

Isotopic labeling studies of the CVD system using $^{15}NH_3$ and $ND_3$ have demonstrated the formation of $Ti^{15}N$ and the use of $ND_3$ gives $DNMe_2$.[11] These observations are strong support for a gas-phase transamination reaction and also explain the need for $NH_3$ to produce low-carbon films. Reaction with $NH_3$ effectively removes $HNMe_2$ from the precursor thereby reducing the carbon content of TiN presumably through the formation of a reactive intermediate that decomposes on the surface. Surface reaction in the absence of gas-phase reactions ($<10^{-5}$ Torr) has been shown to give low-carbon TiN from $Ti(NMe_2)_4$ and $NH_3$, apparently from a transamination reaction on the surface.[15] However, this is quite different from the high pressure conditions (>10 Torr) found in the CVD process.

There is some evidence that, in addition to determining the purity of TiN, the chemistry of the process also affects its step coverage, resistivity, and morphology. It has been reported that $Ti(NEt_2)_4$ gives higher quality TiN than $Ti(NMe_2)_4$.[12] Indeed, these workers found that the TiN produced with $Ti(NMe_2)_4$ was unacceptable with high, unstable resistivity, poor step coverage, and morphology. Apparently, the rate of reaction of $Ti(NMe_2)_4$ with $NH_3$ is too fast and leads to the formation of intermediates with high sticking coefficients or low surface mobility.[16] The reaction of $Ti(NEt_2)_4$ with $NH_3$ is much slower and is the likely reason for the improved film properties. This is particularly intriguing because it indicates that, by controlling the reaction rates, it may be possible to control the step coverage and other properties of TiN.

The work described herein focuses on the gas-phase kinetics of the reaction of $Ti(NMe_2)_4$ with $NH_3$. We are particularly interested in the relationship between gas-phase chemistry and the properties of materials produced by CVD. The primary goal of this work is to obtain a better fundamental understanding of this reaction that is critical to the successful production of TiN films by CVD. An additional goal is to obtain accurate kinetics data that can be used in quantitative numerical models to aid the design of optimized CVD reactors. Below data are presented which satisfy both of these objectives, some of which have been published in preliminary form.[17] Accurate values for the rate constant for reaction of $Ti(NMe_2)_4$ with $NH_3$ are presented including the room temperature isotope effect with $ND_3$ as well as the temperature dependence. The rate constant is not affected by mass transport effects, wall reactions, or total pressure. However, the reaction rate with $NH_3$ is inhibited by the addition of excess $HNMe_2$. The proposed mechanism is the reversible initial transamination reaction, $Ti(NMe_2)_4 + NH_3 \rightleftarrows (Me_2N)_3Ti-NH_2 + HNMe_2$, followed by elimination of $HNMe_2$ from $(Me_2N)_3Ti-NH_2$ to form $(Me_2N)_2Ti{=}NH$. From the dependence of the observed rate constants on $HNMe_2$, the branching ratio for reaction of $(Me_2N)_3Ti-NH_2$ with $HNMe_2$ versus elimination of $HNMe_2$ is obtained. In addition to providing important mechanistic insight, the use of amines may provide a simple method to control the reaction of amido precursors with $NH_3$ to improve the properties of TiN and related nitride materials.

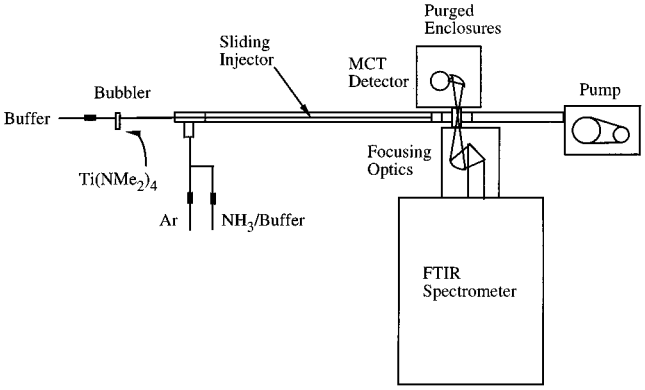


**Figure 1.** Flow-tube reactor (FTR) interfaced to the FTIR spectrometer.

## Experimental Section

The experimental apparatus used to examine the gas-phase kinetics is a flow tube reactor shown in Figure 1. It is a 1-m-long, 1.37-in.-i.d. Teflon-coated stainless-steel tube equipped with a sliding injector port that provides a variable distance from the focus of the IR beam. The injector is a 1/4-in. tube ending in a Pyrex loop with many equally spaced holes for gas injection counter-current to the main flow for good mixing. The observation region is a standard cross (NW-40) equipped with purged windows, purged capacitance manometers, and a throttle valve controller to maintain constant pressure. A tubular Teflon insert with 0.75-in.-diameter holes aids in separating the reactive flows from the IR windows. Argon is used as the purge gas to reduce diffusion and the build up of deposits on the windows. Both the flow tube and the observation region are wrapped with heat tape for elevated temperature operation when desired. The IR beam from the FTIR spectrometer (Nicolet 800) is focused in the middle of the observation region using a combination of flat and off-axis parabolic mirrors. A detector module with focusing mirror is mounted on the opposite side of the flow tube. The focusing optics and the detector module are enclosed in Plexiglas boxes and the entire beam path is purged with dehumidified, $CO_2$-free air. Mass flow meters measure the separate flows of buffer (Ar or He), carrier (Ar or He), and purge (Ar) gases, $NH_3$, and $HNMe_2$. Dilute mixtures of $NH_3$ (9.77%) and $HNMe_2$ (16.6%) in He were used. The flow meters were calibrated by monitoring the pressure rise in a known volume as a function of time. The buffer gas, $NH_3$, and $HNMe_2$ flows were mixed and fed into the side arm of the flow tube. A mixture of $Ti(NMe_2)_4$ in buffer gas, generated from a glass bubbler at ambient temperature, flowed through the sliding injector. A mechanical pump (Sergeant Welch 1397) was equipped with a liquid nitrogen trap for pumping. The Reynolds numbers for these experiments are typically around 10, well within the laminar flow regime.[18]

For the $O_3$ experiment, a mixture of He and $O_2$ flowed into an ozone generator and then into the sliding injector of the flow tube. (***Warning:*** *Condensed ozone is an explosion hazard, do not use a liquid nitrogen trap with ozone.*) We routinely generated a mixture of 1.4% $O_3$ in $O_2$ and He. This was confirmed by IR absorption using the integrated absorbance of the 1042-$cm^{-1}$ band and the accepted integrated band

(13) Sugiyama, K.; Pac, S.; Takahashi, Y.; Motojima, S. *J. Electrochem. Soc.* **1975**, *122*, 1545−1549.

(14) (a) Bradley, D. C.; Gitlitz, M. H. *J. Chem. Soc. (A)* **1969**, 980−984. (b) Bradley, D. C.; Torrible, E. G. *Can. J. Chem.* **1963**, *41*, 134−138. (c) Bradley, D. C.; Thomas, I. M. *J. Chem. Soc.* **1960**, 3857−3861.

(15) Truong, C. M.; Chen, P. J.; Corneille, J. S.; Oh, W. S.; Goodman, D. W. *J. Phys. Chem.* **1995**, *99*, 8831−8842.

(16) (a) Hsieh, J. J. *J. Vac. Sci. Technol. A* **1993**, *11*, 78−86. (b) Rey, J. C.; Cheng, L.-Y.; McVettie, J. P.; Saraswat, K. C. *J. Vac. Sci. Tech.* **1991**, *A9*, 1083.

(17) (a) Weiller, B. H. *Mater. Res. Soc. Symp. Proc.* **1993**, *282*, 605−610. (b) Weiller, B. H.; Partido, B. V. *Chem. Mater.* **1994**, *6*, 260−261. (c) Weiller, B. H. *Mater. Res. Soc. Symp. Proc.* **1994**, *335*, 159−164. (d) Weiller, B. H. *Mater. Res. Soc. Symp. Proc.* **1994**, *334*, 379−384. (e) Weiller, B. H. *Chem. Mater.* **1995**, *7*, 1609−1611.

(18) Welty, J. R.; Wicks, C. E.; Wilson, R. E. *Fundamentals of Momentum, Heat and Mass Transfer*; John Wiley & Sons: New York, 1984.

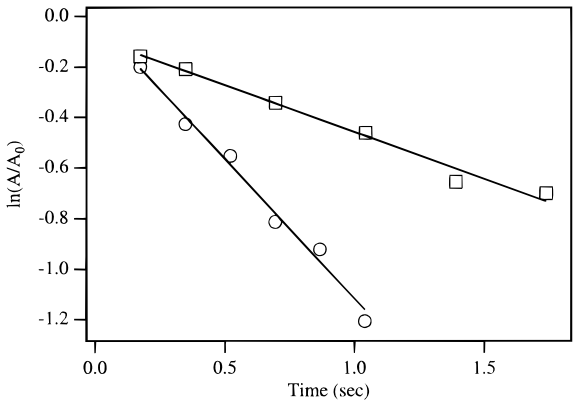


**Figure 2.** Plot of $\ln(A/A_0)$ vs time for the reaction of $O_3$ with isobutene. The squares and circles are for 1.15 and 2.32 Torr of isobutene, respectively.

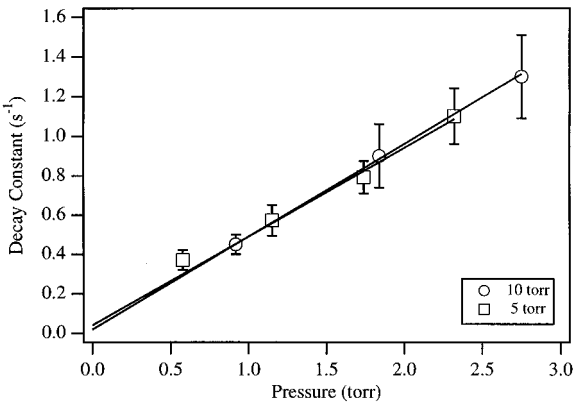


**Figure 3.** Plot of the observed decay constants ($k_{obs}$) vs isobutene partial pressure for the reaction of $O_3$ with isobutene. The total pressure is indicated in the legend.

intensity.[19] Isobutene flowed into the side arm of the flow tube along with the buffer gas.

After an extended number of runs with $Ti(NMe_2)_4$ and $NH_3$, a tan deposit formed on the walls of the flow tube reactor. A similar deposit was noted in earlier work and an IR spectrum was reported.[11a] In order to remove this deposit and obtain a clean Teflon surface, a fluorine plasma was used to clean the flow tube *ex situ*. This procedure was very effective in removing the deposit and resulted in either a clean surface or a powdery white residue that could be wiped off easily. Presumably this white substance is $TiF_x$, which has been noted to sublime readily at elevated temperatures.[20]

The following chemicals were used as received from the indicated suppliers: $Ti(NMe_2)_4$ (Schumacher); $Ti(NEt_2)_4$ (Schumacher); Ar (Spectra Gases, UHP grade); $NH_3$ (Matheson, electronic grade), $ND_3$ (Cambridge Isotope Labs), He (Spectra Gases, UHP grade), $O_2$ (Airco), isobutene, (Aldrich), $NF_3$ (Matheson, electronic grade), and $HNMe_2$ (Aldrich). The spectrometer was operated at 8-$cm^{-1}$ resolution and 256 scans were averaged unless noted. For kinetics measurements integrated intensities were used.

## Results

**A. Kinetics of a Known Reaction: $O_3$ + Isobutene.** The decay of $O_3$ was measured as a function of reaction time as shown in Figure 2. The IR absorbance of $O_3$ was monitored by the $\nu_3$ band at 1042 $cm^{-1}$.[19] The isobutene pressure ranged from 0.5 to 2.3 Torr and is in far excess over the $[O_3]$. Therefore pseudo-first-order conditions apply and we expect an exponential decay of $O_3$: $[O_3] = [O_3]_0 \exp(-k_{bi}[C_4H_8]t)$, where $k_{bi}$ is the bimolecular rate constant. Furthermore, we expect a linear relationship between the logarithm of the IR absorbance and the reaction time: $\ln(A/A_0) = -k_{obs}t$, $k_{obs} = k_{bi}[C_4H_8]$. Here $A$ is the integrated absorbance of the $O_3$ band, $A_0$ is the integrated absorbance of the $O_3$ band in the absence of isobutene (average of initial and final values), $k_{obs}$ is the observed decay constant, and $k_{bi}$ is the bimolecular rate constant. Figure 2 shows such a linear dependence for two isobutene pressures. The slopes of the lines in Figure 2 ($k_{obs}$) should show a linear dependence on isobutene partial pressure. Figure 3 shows this expected result and provides the bimolecular rate constant, $k_{bi} = (13.8 \pm 0.1) \times 10^{-16}$ molecules$^{-1}$ cm$^3$ s$^{-1}$ at 25 °C and 10 Torr total pressure. Figure 4 also shows that when the total pressure is changed to 5 Torr, there is no significant effect on the rate constant.

**B. Room Temperature Kinetics of $Ti(NMe_2)_4$ + $NH_3$.** Figure 4 shows the IR spectra obtained when $Ti(NMe_2)_4$ is reacted with $NH_3$ in a static cell at room temperature. The top spectrum shows $Ti(NMe_2)_4$ alone, the next spectrum is just after (<7 s) the addition of 27.6 Torr of a mixture of 13.8% $NH_3$ in He, and the third spectrum is after no further changes were observed. At the bottom is a reference spectrum for a sample of dimethylamine. From this we can clearly see that dimethylamine is formed from the reaction of $Ti(NMe_2)_4$ with $NH_3$ as observed by Dubois et al.[11] The reaction between $Ti(NMe_2)_4$ and $NH_3$ is too fast to be measured in the static cell and the flow tube reactor is needed for this.

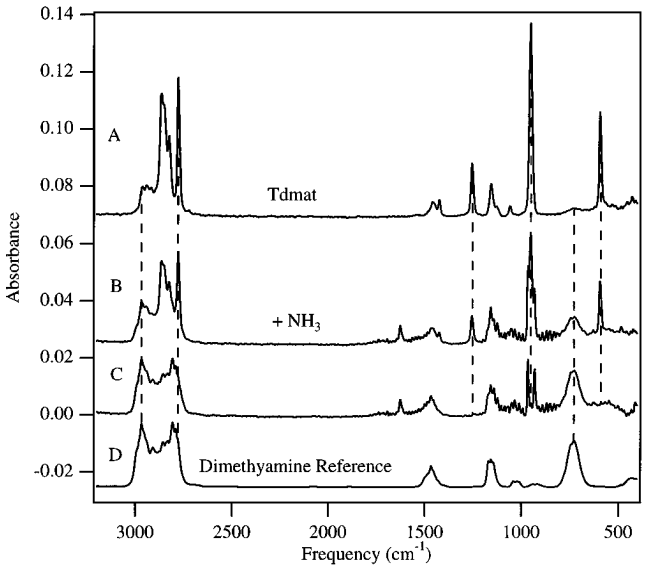


**Figure 4.** IR spectra of the reaction of $Ti(NMe_2)_4$ with $NH_3$ in the static cell: (A) initial spectrum of $Ti(NMe_2)_4$ alone, (B) ~7 s after addition of $NH_3$, (C) after complete reaction, and (D) reference spectrum for $HNMe_2$. The dashed lines indicate major features of $Ti(NMe_2)_4$ and $HNMe_2$.

Figure 5 shows the IR spectra obtained when $Ti(NMe_2)_4$ is reacted with $NH_3$ in the flow tube reactor. The top spectrum (A) is in the absence of $NH_3$. The relatively intense $NC_2$ symmetric stretch at 950 $cm^{-1}$ is a good signature for $Ti(NMe_2)_4$,[21] and we use it to monitor the number density of $Ti(NMe_2)_4$. The middle four spectra result from the addition of 0.245 Torr of $NH_3$ and increasing the distance between the injector and observation region from 10 to 80 cm at constant $NH_3$ pressure. The flow rate was 170 sccm giving the reaction times listed in the caption. In spectra B through E, we see $NH_3$ bands at 968 and 932 $cm^{-1}$ ($\nu_2$) and at 1628 $cm^{-1}$ ($\nu_4$).[22] These

(19) Pugh, L. A.; Rao, K. N. Intensities from Infrared Spectra. In *Molecular Spectroscopy: Modern Research*; Academic: New York, 1976; Vol. II, p 165f.

(20) Cotton, F. A.; Wilkinson, G. *Advanced Inorganic Chemistry*, 4th ed.; Wiley: New York, 1980; p 692.

(21) van der Vis, M. G. M.; Konings, R. J. M.; Oskam, A.; Walter, R. *J. Mol. Struct.* **1994**, *323*, 93−101.

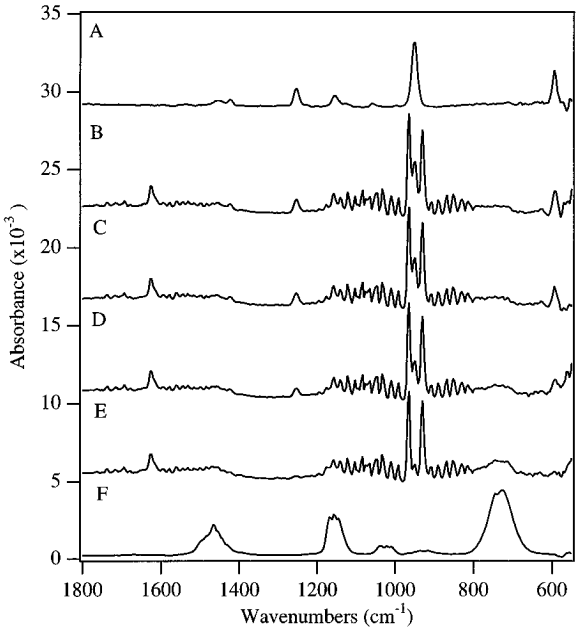


**Figure 5.** IR spectra for the reaction of $Ti(NMe_2)_4$ with $NH_3$ in the flow tube reactor. The top spectrum (A) is prior to $NH_3$ addition and the bottom spectrum (F) is for a sample of $HNMe_2$. Spectra B through E result from the addition of 0.245 Torr of $NH_3$ to the sample in (A) and the following reaction times: (b) 0.69, (c) 1.37, (d) 2.75, (e) 5.49 s.

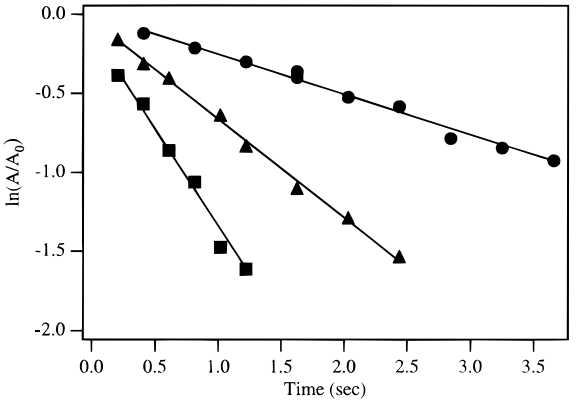


**Figure 6.** Plot of $\ln(A/A_0)$ vs time for the reaction of $Ti(NMe_2)_4$ with $NH_3$. The $NH_3$ pressures are 0.090 (●), 0.179 (▲), and 0.357 (■) Torr.

spectra clearly show the disappearance of $Ti(NMe_2)_4$ with increasing reaction time. The bottom spectrum is for a sample of $HNMe_2$ at 8-$cm^{-1}$ resolution and by comparison we can clearly see the formation of $HNMe_2$. It should be noted that these results are not limited by mixing rates (see below) and therefore $HNMe_2$ is a direct product from the reaction of $NH_3$ with $Ti(NMe_2)_4$.

Figure 6 shows that when the integrated intensity of the 950 $cm^{-1}$ band is plotted vs time on a semilog plot, a linear dependence is observed as expected for a pseudo-first-order reaction. From the available vapor pressure data,[23] the estimated $Ti(NMe_2)_4$ partial pressure is ~0.01 Torr and is much less than the $NH_3$ pressure (0.1−0.4 Torr). Therefore a simple exponential decay is expected: $[Ti(NMe_2)_4] = [Ti(NMe_2)_4]_0 \exp(-k_1[NH_3]t)$, where $k_1$ is the bimolecular rate constant. As

(22) Herzberg, G. *Infrared and Raman Spectra of Polyatomic Molecules*, 1st ed.; Van Nostrand Reinhold Company: New York, 1945; p 295.

(23) (a) The vapor pressure curve for $Ti(NMe_2)_4$ is $\log(P_{torr}) = 8.60 - 2850/T$, or at 25 °C it is $P = 0.11$ Torr: Roberts, D. The Schumacher Corporation. Personal communication. (b) Similar data can be found in: Intemann, A.; Koerner, H.; Koch, F. *J. Electrochem. Soc.* **1993**, *140*, 3215−3222.

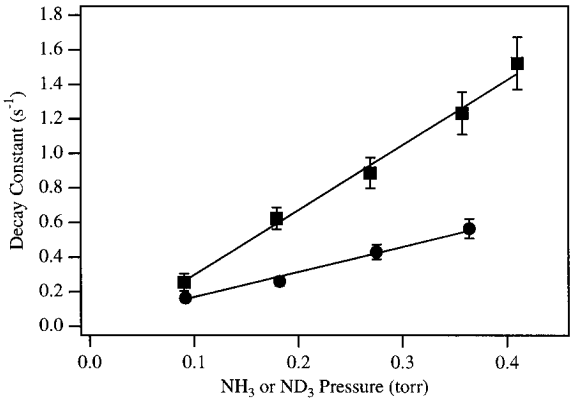


**Figure 7.** Plot of the observed decay constants ($k_{obs}$) vs $NH_3$ (■) and $ND_3$ (●) pressure. He buffer gas was used.

discussed above for $O_3$, a plot of the logarithm of the IR absorbance vs the reaction time should be linear: $\ln(A/A_0) = -k_{obs}t$, $k_{obs} = k_1[NH_3]$, where $A$ is now the integrated absorbance of the $Ti(NMe_2)_4$ band. In a time-dependent experiment, $A_0$ would be the absorbance at zero time. We cannot obtain $A_0$ this way since at zero time (distance) the injector would block the IR beam. Instead we substitute the $NH_3$ flow with buffer gas and measure the $Ti(NMe_2)_4$ absorbance. This is equivalent since we have shown that in the absence of $NH_3$, there is no dependence of the $Ti(NMe_2)_4$ absorbance on the position of the injector over the length of the flow tube (see below). $A_0$ is recorded before and after each kinetic run to confirm that there has been no change in the $Ti(NMe_2)_4$ concentration due to bubbler fluctuations. The experiment was repeated for a series of $NH_3$ pressures. The data were fit to straight lines using a weighted least-squares routine and the slopes of these lines give the observed decay constants ($k_{obs}$) at each $NH_3$ pressure. When the observed decay constants ($k_{obs}$) are plotted against $NH_3$ pressure (Figure 7), we find a linear dependence with a zero intercept as expected for pseudo-first-order conditions. The slope of this plot gives the bimolecular rate constant $k_1 = (1.2 \pm 0.2) \times 10^{-16}$ molecules$^{-1}$ cm$^3$ s$^{-1}$.

**C. Effects of Buffer Gas, Total Pressure, and Flow Velocity.** The effects of buffer gas, total pressure and flow velocity on the reaction kinetics were examined. In order to test for the possibility that the observed rates are affected by the mixing rates, the effect of buffer gas on these measurements was studied. The calculated diffusional mixing time at 25 °C is about three times longer in Ar than in He (see below). If the mixing time was significant, this would be reflected in a smaller observed rate constant in Ar. When the measurements were repeated in Ar buffer gas, the observed bimolecular rate constant is well within experimental error of the He value. The effect of total pressure was also investigated. When the total pressure was varied from 10 to 20 Torr with the linear flow velocity held constant at 24 cm/s, there is no significant difference in the observed rate constants. Furthermore, when the linear flow velocity was changed by a factor of 2 from 24 to 49 cm s$^{-1}$ at constant pressure (10 Torr), no change in the decay constants was observed.

**D. Kinetics of $Ti(NMe_2)_4$ + $ND_3$.** In order to gain some insight into the reaction mechanism, the kinetics of $Ti(NMe_2)_4$ with $ND_3$ were examined. Since the transamination reaction involves cleavage of an N−H bond, we would expect a significant kinetic isotope effect with $ND_3$ if this is the rate-limiting step. When $ND_3$ is used instead of $NH_3$, good pseudo-first-order kinetics are observed as shown in Figure 8. When the decay constants are plotted against $ND_3$ pressure, the rate constant is reduced substantially from the $NH_3$ value. Figure

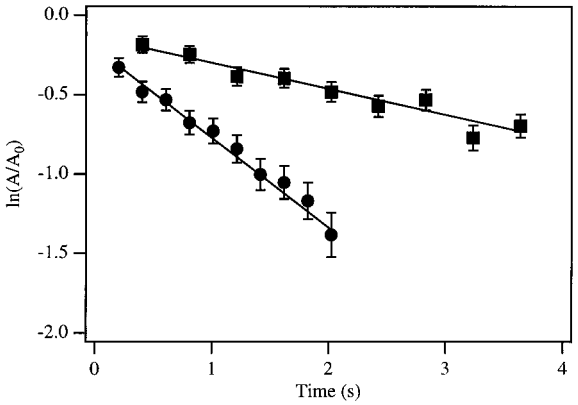


**Figure 8.** Plot of $\ln(A/A_0)$ vs time for the reaction of $Ti(NMe_2)_4$ with $ND_3$ using He buffer gas. The $ND_3$ pressures are 0.0915 (■) and 0.364 (●) Torr.

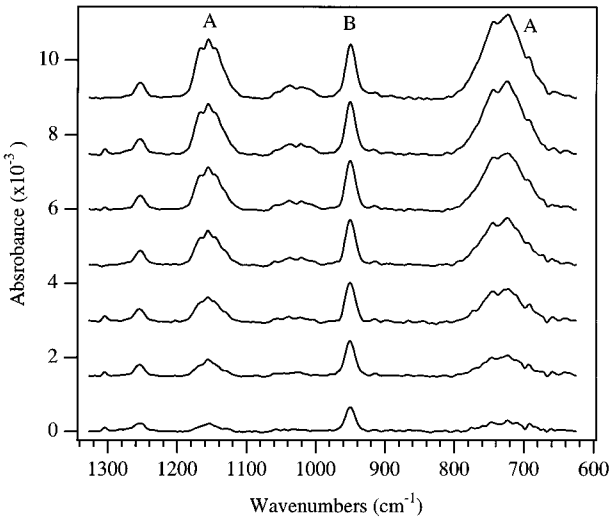


**Figure 9.** IR spectra of the reaction of $Ti(NMe_2)_4$ with $NH_3$ as a function of added $HNMe_2$. The $NH_3$ was held constant at 0.46 Torr and the $HNMe_2$ pressure was varied from 0 (bottom) to 0.298 (top) Torr. Features are marked with A for $HNMe_2$ and B for $Ti(NMe_2)_4$. Each spectrum is offset by $1.5 \times 10^{-3}$ absorbance units.

7 shows this plot along with the corresponding $NH_3$ data. The $ND_3$ rate constant is $k_d = (4.5 \pm 0.5) \times 10^{-17}$ molecules$^{-1}$ cm$^3$ s$^{-1}$ giving an isotope effect ratio of $k_H/k_D = 2.4 \pm 0.4$. This indicates a primary isotope effect and that H-atom transfer is involved in the rate-limiting step of this reaction. This is consistent with labeling studies that showed the amine proton in the product $HNMe_2$ originates from $NH_3$.[11] Below we discuss the mechanistic implications of this result.

**E. Effect of Dimethylamine on the Kinetics.** The IR spectra when $Ti(NMe_2)_4$ is reacted with $NH_3$ in the presence of $HNMe_2$ are shown in Figure 9. The reaction time was 0.60 s as determined by the injector position (30 cm) and the flow velocity (49.7 cm s$^{-1}$). The partial pressure of $HNMe_2$ was varied (0, 0.051, 0.098, 0.148, 0.198, 0.248, and 0.297 Torr) while the total and $NH_3$ flows were held constant ($NH_3 = 0.46$ Torr). The bands at 1156 and 730 cm$^{-1}$ (A) are both for $HNMe_2$ ($CH_3$ rock and NH bend, respectively)[24] and the band at 950 cm$^{-1}$ (B) is the $NC_2$ stretch for $Ti(NMe_2)_4$. Reference spectra for $NH_3$ acquired under similar experimental conditions were used to subtract the $NH_3$ bands. In the initial spectrum the extent of reaction is about 75% as measured by the amount of $Ti(NMe_2)_4$ remaining. When the partial pressure of $HNMe_2$ is increased at constant $NH_3$ pressure (0.46 Torr) and flow

(24) Gamer, G.; Wolff, H. *Spectrochim. Acta* **1973**, *29A*, 129.

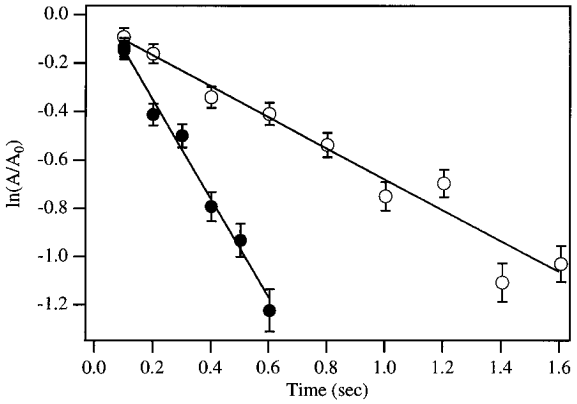


**Figure 10.** Effect of $HNMe_2$ on the reaction rate of $Ti(NMe_2)_4$ with $NH_3$. The slope is $k_{obs}$ and the open points have added $HNMe_2$ (0.198) and the solid points do not.

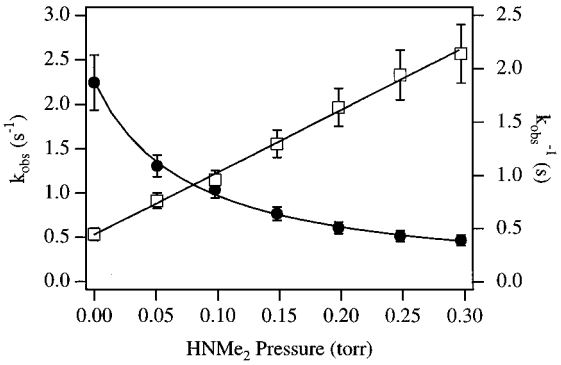


**Figure 11.** The dependence of $k_{obs}$ (●) and $(k_{obs})^{-1}$ (□) on $HNMe_2$ pressure. The $NH_3$ pressure was held constant at 0.46 Torr.

conditions, the concentration of $Ti(NMe_2)_4$ clearly increases. At the highest $HNMe_2$ pressure used, there is about a 3-fold increase in $[Ti(NMe_2)_4]$ or an extent of reaction of only 25%. When sufficient $HNMe_2$ is added to the gas stream, the reaction of $Ti(NMe_2)_4$ with $NH_3$ is substantially inhibited over this time scale.

The decay rates of $Ti(NMe_2)_4$ with and without added $HNMe_2$ are shown in Figure 10. The $NH_3$ pressure was 0.46 Torr and the data are plotted as $\ln(A/A_0)$ vs time. Pseudo-first-order conditions apply for both data sets and the semilog plots are linear. The rate constant ($k_1$) is calculated from the slope ($k_{obs}$) and the $NH_3$ pressure where $k_{obs} = k_1(NH_3)$. In the absence of $HNMe_2$, the rate constant is the same within experimental error as that observed earlier, $k_1 = (1.4 \pm 0.2) \times 10^{-16}$ cm$^3$ molecules$^{-1}$ s$^{-1}$. In the presence of 0.198 Torr of $HNMe_2$, the rate constant is reduced significantly to $k_1 = (0.43 \pm 0.03) \times 10^{-16}$ cm$^3$ molecules$^{-1}$ s$^{-1}$. In an independent confirmation of this result, we have also examined the reaction rates of $Ti(NMe_2)_4$ with $NH_3$ in a static cell. Again we find that the addition of $HNMe_2$ significantly reduces the reaction rates.

Using data from Figure 9, $k_{obs}$ was calculated from $\ln(A/A_0)$ and the reaction time. The resulting values for $k_{obs}$ are plotted in Figure 11 showing that $k_{obs}$ is inversely dependent on the $HNMe_2$ pressure. Also plotted is $(k_{obs})^{-1}$, showing a linear dependence on $HNMe_2$ pressure. Figure 12 shows that the dependence of $k_{obs}$ on $NH_3$ pressure in the presence of 0.297 Torr of $HNMe_2$ is linear.

**F. Temperature Dependence.** We have obtained data on the temperature dependence of the rate constant for the removal of $Ti(NMe_2)_4$ by ammonia. To accomplish this, the bubbler was operated at room temperature and the flow tube was wrapped with heat tape and heated with temperature controllers. We have already demonstrated that the dependence of $k_{obs}$ on

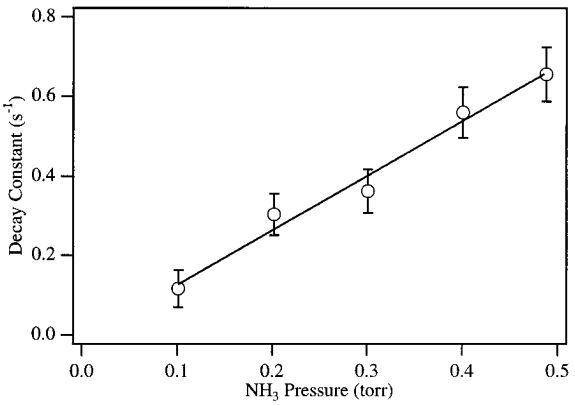


**Figure 12.** Dependence of $k_{obs}$ on $NH_3$ in the presence of $HNMe_2$. The $HNMe_2$ pressure is 0.297 Torr.

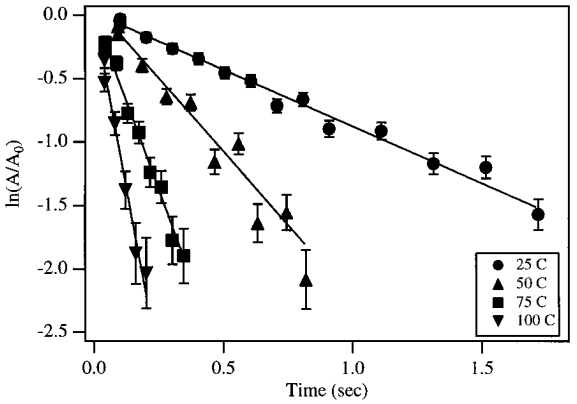


**Figure 13.** Temperature dependence of the $Ti(NMe_2)_4$ removal rates. The $NH_3$ densities are listed in Table 1.

**Table 1.** Kinetics Data for $Ti(NMe_2)_4 + NH_3$

| $T$ (°C) | $k_{obs}$ ($s^{-1}$) | $NH_3$ ($10^{15}$ $cm^{-3}$) | $k$ ($10^{-16}$ $cm^3$ $s^{-1}$) |
|---|---|---|---|
| 25.0 | 0.894 ± 0.03 | 7.43 | 1.20 ± 0.04 |
| 50.0 | 2.31 ± 0.1 | 6.87 | 3.4 ± 0.1 |
| 75.0 | 5.54 ± 0.3 | 6.38 | 8.7 ± 0.5 |
| 100.0 | 11.0 ± 1.1 | 5.95 | 18.5 ± 2.0 |

$NH_3$ is first order. Therefore, we determined the observed decay constant at a single $NH_3$ pressure (0.230 Torr) at each of four temperatures, 25, 50, 75, and 100 °C. Figure 13 shows the decay plots for $Ti(NMe_2)_4$ at each of these temperatures. The slopes ($k_{obs}$) of these plots are shown in Table 1 along with the $NH_3$ densities and the calculated bimolecular rate constants.

Figure 14 shows an Arrhenius plot of the log of the rate constants against inverse temperature. The slope and intercept of this plot give values of the activation energy $E_a$ and $A$ factor as follows: $E_a = 8.1 \pm 0.1$ kcal/mol and $\log(A) = -10.0 \pm 0.2$ The error bars are the statistical result from the fitting procedure. While this temperature range is less than the limit to the experimental apparatus (~200 °C), it was not possible to go to higher temperatures given the signal-to-noise ratio of the data. Higher temperatures would require better time resolution (higher flow velocity) that would result in greater dilution by buffer gas. In any event, the excellent precision of the data allows reliable extrapolations to higher temperatures.

## Discussion

In order to confirm that the flow tube reactor produces reliable kinetics data, we have measured the rate constant for the reaction of $O_3$ with isobutene. This reaction was selected for several reasons: (1) a reliable value is available since this reaction is

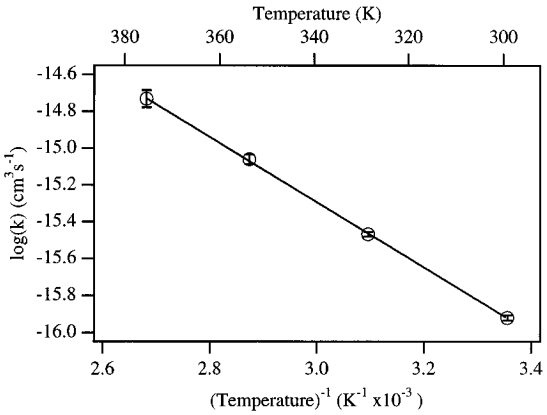


**Figure 14.** Temperature dependence of the rate constant ($k_1$) for $Ti(NMe_2)_4 + NH_3$.

important in atmospheric chemistry and it has been measured numerous times over the years by several different techniques,[25] (2) the rate constant is close in magnitude to the value for $Ti(NMe_2)_4 + NH_3$, and (3) the IR absorption bands of isobutene are sufficiently removed from the $O_3$ band at 1042 $cm^{-1}$ to avoid overlap.

As Figures 2 and 3 show, we find the rate constant is (13.8 ± 0.1) × $10^{-18}$ $molecules^{-1}$ $cm^3$ $s^{-1}$ at 25 °C and 10 Torr total pressure. This is in excellent agreement with the best literature value for this reaction of (13.6 ± 0.2) × $10^{-18}$ $molecules^{-1}$ $cm^3$ $s^{-1}$.[25] This is particularly significant since very different conditions and techniques were used previously—a static sample at a total pressure of 760 Torr and *ex situ* measurement of the $O_3$ concentration. The fact that we are able to reproduce this rate constant is important. A serious concern in flow tube studies is the rate of mixing of the two reagents to produce a homogeneous mixture. For very fast reactions this can be rate limiting and can prevent measurement of the reaction rate constant. The fact that there is no dependence on total pressure is also significant since the diffusional mixing time differs by a factor of 2 between these two pressures. This observation coupled with the good agreement with the literature clearly demonstrates that mixing is not rate limiting under these conditions and confirms the reliability of our kinetics data.

The flow tube kinetics data in Figure 5 show the direct, rapid reaction of $Ti(NMe_2)_4$ with $NH_3$ to produce $HNMe_2$. We have shown that our kinetics are not determined by mixing rates through several sets of results. First, the rate constants are not affected by changing the buffer gas from He to Ar which would increase the diffusional mixing time by a factor of 3.2 from 0.07 and 0.2 s in He and Ar, respectively, at 25 °C.[26] The diffusion constant in He was estimated to be 8.9 $cm^2$ $s^{-1}$ at 298 K and 10 Torr from a collision radius for $Ti(NMe_2)_4$ of 4.5 Å and the mixing times were calculated as described elsewhere.[27] This calculation is an upper bound and the actual mixing times will be significantly shorter when turbulence and off-axis flow velocity are considered. The shortest observation time is 0.05 s and mixing should not be significant for these measurements. Second, when the total pressure is varied from 10 to 20 Torr, which would increase the mixing time by a factor of 2, there is no effect on the observed reaction rates. Finally, we observe a significant isotope effect which clearly shows that the rates cannot be determined by mass transport. Therefore mixing is not rate limiting under these experimental conditions and the kinetics are chemically controlled. This conclusion is

(25) Japar, S. M.; Wu, C. H.; Niki, H. *J. Phys. Chem.* **1974,** *78,* 2318.
(26) Hirschfelder, J. O.; Curtiss, C. F.; Bird, R. B. *Molecular Theory of Gases and Liquids*; Wiley: New York, 1954.
(27) Keyser, L. F. *J. Phys. Chem.* **1984**, *88,* 4750−4758.

also supported by our ability to reproduce the literature rate constant for the reaction of $O_3$ with isobutene.

There is no evidence for surface reactions of $Ti(NMe_2)_4$ with the Teflon-coated walls of the flow tube reactor. The measured rate constant, $(1.2 \pm 0.2) \times 10^{-16}$ molecules$^{-1}$ cm$^3$ s$^{-1}$, is relatively small and a large number of collisions between $Ti(NMe_2)_4$ and the walls of the flow tube reactor will occur prior to reaction with $NH_3$. Therefore the removal of $Ti(NMe_2)_4$ along the length of the flow tube in the absence of $NH_3$ was examined. The IR intensity of the $Ti(NMe_2)_4$ bands is invariant to the position of the injector over the length of the tube, and consequently the reaction between $Ti(NMe_2)_4$ alone and the Teflon-coated walls of the reactor is negligible. Furthermore, if there was a significant component of wall reaction, one would expect a non-zero intercept for $\ln(A/A_0)$ against time. Figures 6, 8, and 10 show this is not the case, and therefore we conclude that wall reactions do not contribute significantly to the measured rate constant.[28] They may occur but the gas-phase reaction is much faster.

The pressure dependence of the rate constant for the reaction of $Ti(NMe_2)_4$ with $NH_3$ was also measured for two purposes. First the existence of a pressure dependence would provide mechanistic clues about the reaction. Second, modeling efforts include both low-pressure (LPCVD)[29] and atmospheric pressure (APCVD) systems,[30] and therefore it is important to determine if the rate constant determined at low pressure would be valid at higher total pressures. When data like that in Figure 7 are obtained at both 10.0 and 20.0 Torr, there is no significant difference in the slope of the two fits. Therefore we conclude that there is no pressure dependence of the rate constant over this pressure range. A pressure dependence might be observed if collisional quenching of a vibrationally excited intermediate is important in the reaction mechanism. However, this is not likely given the relatively large size of the molecules involved and that a second product is formed that can carry excess energy away. This is supported by the observed independence of the rate constant on buffer gas since Ar is a much more efficient quencher than He. Given the lack of a pressure dependence in this range, it is very unlikely that one would be observed at greater total pressures.

The fact that we have successfully measured the gas-phase rate constant for the reaction of $Ti(NMe_2)_4$ with $NH_3$ is significant. This is apparently the first measurement of the rate constant for a transamination reaction of any metal amide in either gas phase or solution. Previous workers observed the time-dependent removal of $Ti(NMe_2)_4$ by reaction with $NH_3$; however, the rates were determined by mass transport in that study.[11] The calculated gas kinetic rate constant for this reaction is $5 \times 10^{-10}$ cm$^3$ molecules$^{-1}$ s$^{-1}$ and the rate constant represents a small ($2 \times 10^{-7}$) reaction probability. However, it is larger than expected considering the low temperature (24 °C) and that both $Ti(NMe_2)_4$ and $NH_3$ are closed-shell, stable molecules. Our result shows that $Ti(NMe_2)_4$ and $NH_3$ react rapidly even at room temperature. For example, in 1 Torr of $NH_3$ the lifetime (1/e) of $Ti(NMe_2)_4$ is only ~1.0 s at room temperature. Clearly under CVD process conditions of several Torr of $NH_3$ and temperatures between 100 and 400 °C, $Ti(NMe_2)_4$ will not survive intact to reach the surface of the growing film.

**Scheme 1.** Proposed Mechanism of the Reaction between $Ti(NMe_2)_4$ and $NH_3$

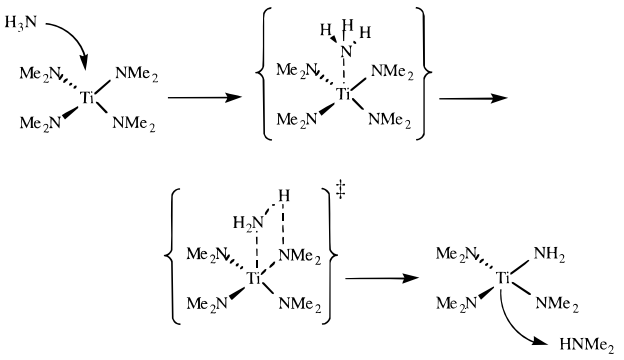


Figures 7 and 8 show the kinetics of the reaction of $Ti(NMe_2)_4$ with $ND_3$ and that an isotope effect of $k_H/k_D = 2.4 \pm 0.4$ is observed. Using transition state theory, the calculated maximum isotope effect for cleavage of an N−H bond in $NH_3$ is $k_H/k_D = 9$ at 298 K.[22,31] The experimental result is consistent with a primary isotope effect due to the zero point energy difference. Therefore N−H bond cleavage is the rate-limiting step. Transamination is consistent with this observation and the probable reaction mechanism is presented in Scheme 1. Initially $NH_3$ could form a weak intermediate adduct with the Ti center in $Ti(NMe_2)_4$. Unlike those formed with $TiCl_4$,[32] this adduct is probably not very stable given the steric bulk of amido ligands and the reduced acidity of the Ti center. H-atom transfer between coordinated $NH_3$ and an amido ligand probably occurs via a four-center transition state followed by elimination of $HNMe_2$.[33] Once the first amido ligand is exchanged, the steric congestion is reduced and subsequent reactions should be faster. Therefore we propose that, in the absence of added $HNMe_2$, the initial transamination reaction is rate limiting. After the initial transamination reaction, elimination reactions could compete with further transaminations. Calculations have found these reactions to be facile as well[34] and we will discuss their potential role below.

The inhibition of the reaction between $Ti(NMe_2)_4$ and $NH_3$ by excess $HNMe_2$ as shown by Figures 9 through 11 has important mechanistic implications. All of the data are consistent with a reversible reaction between $Ti(NMe_2)_4$ and $NH_3$. This is not surprising when one considers the thermochemistry of transamination reactions. The Ti−$NR_2$ bond energies are independent of R to first approximation[35] and the calculated bond energy for Ti−$NH_2$ is close the measured values for Ti−$NR_2$.[36] Since the entropies of the free amines are similar, $\Delta S \sim 0$, the free energy change for the transamination reactions is also approximately zero, $\Delta G \sim 0$. This is consistent with the early studies of transamination reactions of $Ti(NR_2)_4$ with numerous dialkylamines in solution.[14] Others have examined

(28) Under conditions where a large amount of deposit has accumulated on the walls of the flow tube reactor, we find that the rate constants are significantly higher. When the walls are cleaned as described in the Experimental Section, the rate constants return to the quoted value. Prior to each run, the rate constant was measured under control conditions to confirm the lack of wall effects.

(29) Cale, T. S.; Chaara, M. B.; Raupp, G. B.; Raijmakers, I. J. *Thin Solid Films* **1993**, *236*, 294−300.

(30) Toprac, A. J.; Wang, S.-Q.; Musher, J.; Gordon, R. G. *Mater. Res. Soc. Symp. Proc.* **1994**, 236.

(31) Moore, J. W.; Pearson, R. G. *Kinetics and Mechanism*; John Wiley and Sons: New York, 1981.

(32) Saeki, Y.; Masuzaki, R.; Yajima, A.; Akiyama, M. *Bull. Chem. Soc. Jpn.* **1982,** *55*, 3193−3196.

(33) Chisholm, M. H.; Rothwell, I. P. In *Comprehensive Coordination Chemistry*; Wilkinson, G., Ed.; Pergamon Press: New York, 1987.

(34) Cundari, T. R.; Gordon, M. S. *J. Am. Chem. Soc.* **1993**, *115*, 4210−4217.

(35) (a) Lappert, M. F.; Patil, D. S.; Pedley, J. B. *J. Chem. Soc.* **1975**, 830−831. (b) Baev, A. K.; Mikahailov, V. E. *Russ. J. Phys. Chem.* **1989**, *63*, 949−955.

(36) Allendorf, M. D.; Janssen, C. L.; Colvin, M. E.; Melius, C. F.; Nielson, I. M. B.; Osterheld, T.; Ho, P. In *Process Control, Diagnostics, and Modeling in Semiconductor Manufacturing*; The Electrochemical Society: Pennington, NJ, 1995, in press.

the reactions of metal amides with $NH_3$ and observed the irreversible formation of insoluble products.[37] This is not inconsistent with our results since we propose that only the initial transamination reaction to form $(Me_2N)_3Ti-NH_2$ is reversible, not that the overall reaction is at equilibrium. The subsequent, product-forming reactions should be irreversible.

Possible mechanisms for the reaction are shown below. The first step in the proposed mechanism is reversible transamination to form the transient intermediate $(Me_2N)_3Ti-NH_2$ (eq 2). The subsequent reactions are of particular interest since they control which species reach the surface. Two reasonable possibilities are the following: (a) reaction with $NH_3$ in a second transamination step to form $(Me_2N)_2Ti(NH_2)_2$ (eq 3) or (b) elimination of $HNMe_2$ to form an imide (eq 4):

$$Ti(NMe_2)_4 + NH_3 \underset{k_{-1}}{\overset{k_1}{\rightleftharpoons}} (Me_2N)_3Ti-NH_2 + HNMe_2 \quad (2)$$

$$(Me_2N)_3Ti-NH_2 + NH_3 \xrightarrow{k_2} (Me_2N)_2Ti(NH_2)_2 + HNMe_2 \quad (3)$$

$$(Me_2N)_3Ti-NH_2 \xrightarrow{k_3} (Me_2N)_2Ti{=}NH + HNMe_2 \quad (4)$$

The steady state approximation on $(Me_2N)_3Ti-NH_2$ for the two mechanisms, eqs 2 and 3 and 2−4, gives expressions for $k_{obs}$:[38]

$$k_{obs} = \frac{k_1k_2[NH_3]^2}{k_{-1}[HNMe_2] + k_2[NH_3]} \quad (5)$$

$$k_{obs} = \frac{k_1k_3[NH_3]}{k_{-1}[HNMe_2] + k_3} \quad (6)$$

Both expressions give the observed linear dependence of $k_{obs}$ on $NH_3$ when $[HNMe_2] = 0$, $k_{obs} = k_1[NH_3]$, and the derived bimolecular rate constant represents the forward transamination reaction ($k_1$). The observed linear dependence of $(k_{obs})^{-1}$ on $HNMe_2$ is also predicted by both expressions. The distinguishing feature is the order with respect to $NH_3$ in the presence of excess $HNMe_2$: (5) is second order and (6) is first order. The dependence of $k_{obs}$ on $NH_3$ with added $HNMe_2$ (0.297 Torr) was linear with a zero intercept as shown in Figure 12. While this is not conclusive, we favor mechanism 2−4 for several additional reasons. $(Me_2N)_2Ti{=}NH$ could easily give complexes with bridging imido groups similar to those previously postulated as intermediates in this system.[11] A similar imide has been isolated as an intermediate in TiN CVD from $TiCl_4$ and $NH_3$[39] and there are several other related examples as well.[40] Furthermore, a similar reaction sequence has been observed when $Ti(NMe_2)_4$ or $Ta(NMe)_5$ reacts with $Bu^tNH_2$:[41]

$$Ti(NMe_2)_4 + Bu^tNH_2 \rightarrow {}^1/_2[(Me_2N)_2Ti(NBu^t)]_2 \quad (7)$$

$$Ta(NMe_2)_5 + Bu^tNH_2 \rightarrow (Me_2N)_3Ta{=}NBu^t \quad (8)$$

Both of these reactions probably proceed by an initial transamination followed by elimination of $HNMe_2$. Experiments attempting to directly confirm the mechanism are in progress.

This mechanism is consistent with all of our experimental data. There are three sets of data to consider: (1) the dependence of $k_{obs}$ on $NH_3$ (Figure 7), (2) the dependence of $k_{obs}$ on $HNMe_2$ (Figure 11), and (3) the dependence of $k_{obs}$ on $NH_3$ with added $HNMe_2$ (Figure 12). The plot of $(k_{obs})^{-1}$ on $HNMe_2$ in Figure 11 is linear with slope $= 5.86 \pm 0.16$ Torr$^{-1}$ s and intercept $= 0.44 \pm 0.03$ s. The dependence of $(k_{obs})^{-1}$ on $HNMe_2$ predicted by eq 6 is shown below:

$$\frac{1}{k_{obs}} = \frac{k_{-1}[HNMe_2]}{k_1k_3[NH_3]} + \frac{1}{k_1[NH_3]} \quad (9)$$

The product of the intercept and $[NH_3]$ gives $k_1 = (1.5 \pm 0.2) \times 10^{-16}$ molecules$^{-1}$ cm$^3$ s$^{-1}$ which is in good agreement with the value determined from the dependence of $k_{obs}$ on $NH_3$ (Figure 7): $k_1 = (1.2 \pm 0.2) \times 10^{-16}$ molecules$^{-1}$ cm$^3$ s$^{-1}$. From the slope of eq 9, $k_1$, and $[NH_3]$, the calculated value for $(k_3/k_{-1}) = 3.1 \times 10^{15}$ molecules cm$^{-3}$. This quantity enables us to calculate the expected slope for Figure 12 from eq 6, $3.0 \times 10^{-17}$ molecules$^{-1}$ cm$^3$ s$^{-1}$. This is consistent with the observed value, $4.3 \times 10^{-17}$ molecules$^{-1}$ cm$^3$ s$^{-1}$. A relevant quantity to consider is the ratio of first-order rate constants, $k'_{-1}/k_3$, where $k'_{-1}$ is the pseudo-first-order rate constant, $k'_{-1} = k_{-1}[HNMe_2]$. At the $HNMe_2$ pressure used in Figure 12 (0.297 Torr), $k'_{-1}/k_3 = 3.0$, indicating that reaction of $(Me_2N)_3Ti-NH_2$ with $HNMe_2$ is three times as fast as elimination at this $[HNMe_2]$. This supports the proposed mechanism of preequilibrium followed by elimination.

Finally we consider the temperature dependence results in light of this mechanism. In the absence of added $HNMe_2$, $k_{obs} = k_1[NH_3]$ and therefore the bimolecular rate constants are for the initial transamination reaction. Therefore the activation energy $E_a = 8.1 \pm 0.1$ kcal/mol and pre-exponential factor $\log(A) = -10.0 \pm 0.2$ are for this reaction. The calculated activation enthalpy is $\Delta H^\dagger = 6.9 \pm 0.1$ kcal/mol.[31] Unfortunately, literature searches have not uncovered any kinetics data for similar reactions in solution or gas phase for comparison. However, it is useful to consider the magnitude of the pre-exponential factor for consistency with this reaction. The $A$ factor is in good agreement with that expected for a bimolecular metathesis reaction involving polyatomic reactants.[42] A more intuitive interpretation of the $A$ factor is the activation entropy: $\Delta S^\dagger = -19$ cal/(mol K) for a standard state of 1 atm. This is very reasonable for the proposed bimolecular reaction.

It is instructive to compare the activation energy to that derived from CVD studies. The only relevant temperature dependent data on this system comes from one study of TiN deposition from $Ti(NMe_2)_4$ and $NH_3$ at low pressure in a rotating disk reactor (RDR).[43] Most workers have studied this system in standard reactors at higher pressures and have found the deposition rate to be mass transport limited over a wide temperature range with a typical activation energy of 3.5 kcal/mol.[10] However, in the low-pressure RDR study, both transport-limited and kinetically-limited regimes for the deposition rate were found. The kinetically-limited regime below 300 °C gives

(37) (a) Brown, G. M.; Maya, L. *J. Am. Ceram. Soc.* **1988**, *71*, 78−82. (b) Seyferth, D.; Mignani, G. *Mater. Sci. Lett.* **1988**, *7*, 487−488.

(38) Here we have assumed that all subsequent reactions are fast and therefore kinetically unimportant.

(39) (a) Winter, C. H.; Sheridan, P. H.; Lewkebandra, T. S.; Heeg, M. J.; Proscia, J. W. *J. Am. Chem. Soc.* **1992**, *114*, 1095−1097. (b) Lewkebandra, T. S.; Sheridan, P. H.; Heeg, M. J.; Rheingold, A. L.; Winter, C. H. *Inorg. Chem.* **1994**, *33*, 5879−5889.

(40) (a) Hill, J. E.; Profilet, R. D.; Fanwick, P. E.; Rothwell, I. P. *Angew. Chem., Int. Ed. Engl.* **1990**, *29*, 664−665. (b) Roesky, H. W.; Voelker, H.; Witt, M.; Noltemeyer, M. *Angew. Chem., Int. Ed. Engl.* **1990**, *29*, 669−670. (c) Cummins, C. C.; Schaller, C. P.; Van Duyne, G. D.; Wolczanski, P. T.; Chan, A. W. E.; Hoffman, R. *J. Am. Chem. Soc.* **1991**, *113*, 2985−2994.

(41) (a) Nugent, W. A.; Haymore, B. L. *Coord. Chem. Rev.* **1980**, *31*, 123−175. (b) Nugent, W. L.; Harlow, R. L. *J. Chem. Soc., Chem. Commun.* **1978**, 579.

(42) Benson, S. W. *Thermochemical Kinetics*; Wiley: New York, 1976.

(43) Hillman, J. T.; Rice, M. J., Jr.; Studiner, D. W.; Foster, R. F.; Fiordalice, R. W. *Proc. VMIC Conf.* **1992**, 246−252.

an activation energy of 7.5 kcal/mol. This is in excellent agreement with our data and suggests that the transamination reaction is rate limiting in the kinetic regime in the CVD system.

## Conclusions

The reaction between $Ti(NMe_2)_4$ and $NH_3$ is rapid even at room temperature. When $Ti(NMe_2)_4$ is mixed with less than 5 Torr of $NH_3$ in a closed gas cell, the reaction is complete in less than 5 s. The only gas-phase product that could be identified conclusively is $HNMe_2$ and this is consistent with a transamination reaction between $Ti(NMe_2)_4$ and $NH_3$. This explains the importance of $NH_3$ in the formation of low-carbon TiN films; carbon is removed from the starting material through the formation of $HNMe_2$.

We have used a flow tube reactor to measure the kinetics of the gas-phase reaction between $Ti(NMe_2)_4$ and $NH_3$. In the flow tube reactor, the IR spectra show that $Ti(NMe_2)_4$ is completely reacted in 5 s in the presence of 0.1 Torr of $NH_3$ with the formation of $HNMe_2$ as a direct product. The dependence of the decay rates on $NH_3$ pressure gives the rate constant at 24 °C: $k = (1.2 \pm 0.2) \times 10^{-16}$ molecules$^{-1}$ cm$^3$ s$^{-1}$. The use of He or Ar buffer gas has no effect on the value of the rate constant demonstrating that the kinetics are not determined by mass transport. This rate constant is relatively large and confirms quantitatively the rapid reaction between $Ti(NMe_2)_4$ and $NH_3$. For example, the rate constant indicates that in the presence of 1 Torr of $NH_3$, the lifetime of $Ti(NMe_2)_4$ is ~1 s at room temperature. Clearly under the CVD process conditions of high $NH_3$ pressures and temperatures, extensive gas reactions do occur and $Ti(NMe_2)_4$ will be converted into a new species before it reaches the surface of the growing film. In order to understand this and other CVD processes, it is critical to obtain data on the rates of these gas-phase reactions.

The rate constant is independent of total pressure and shows that the rate constant is valid for modeling systems under a range of pressures. In addition, wall reactions do not contribute significantly to the observed reaction rates. When $ND_3$ is used instead of $NH_3$, a normal isotope effect is observed showing that an N−H bond is broken in the rate-limiting step of reaction. Given this result and the observation of dimethylamine as the direct product, we propose that the transamination reaction between $Ti(NMe_2)_4$ and $NH_3$ is the rate-limiting step of the reaction. The rate constant is assigned to the transamination of the first amido ligand. After transamination, elimination to form an imido intermediate is most consistent with the kinetic data and with prior studies. Unfortunately the data do not allow for more detailed identification of the intermediates responsible for film growth. Direct *in situ* spectroscopic studies will be required for this and are planned.

The temperature dependence of the rate constant was determined and provides activation parameters for the rate constant: $\log(A) = -10.0 \pm 0.2$; $E_a = 8.1 \pm 0.1$ kcal/mol. The activation entropy, $\Delta S^\dagger = -19$ cal/(mol K), is consistent with the proposed rate-limiting step of transamination. The precision of the activation parameters is high and allows calculation of the rate constant over a wide range of temperatures for modeling this system. The activation energy is in excellent agreement with the activation energy for the deposition of TiN from $Ti(NMe_2)_4$ and $NH_3$ under kinetically controlled conditions: $E_a = 7.4$ kcal/mol. This is consistent with transamination as the rate-limiting step in the deposition of TiN.

As discussed in the introduction, the properties of TiN deposited from $Ti(NMe_2)_4$ and $NH_3$ are not acceptable and $Ti(NEt_2)_4$ gives much better films. The reaction rate of $Ti(NEt_2)_4$ with $NH_3$ is much slower than for $Ti(NMe_2)_4$[44] and this appears to explain the difference in film properties. One of the most important of these is step coverage, and $Ti(NEt_2)_4$ is much better in this regard than $Ti(NMe_2)_4$. Step coverage is thought to be predominantly controlled by the sticking coefficient of the molecule reacting with the surface. Molecules with low sticking coefficients can survive numerous collisions with the side walls of a feature to react with the bottom and hence will give better step coverage. The large rate constant for $Ti(NMe_2)_4$ means that, under CVD conditions, it will be completely reacted and may be converted into an intermediate that has a large sticking coefficient. In the case of $Ti(NEt_2)_4$, the rate constant is much smaller, the extent of reaction is much smaller, and intermediates with smaller sticking coefficients could be formed.

One of the most significant results of this work is the observation that a transamination reaction between a metal amide and $NH_3$ is reversible, apparently for the first time. This has important implications for the chemistry of amido compounds as well as for the CVD of TiN from them. For example, the use of amines may provide a simple method for controlling the extent of gas-phase reaction and therefore the properties of TiN. In addition, this result will provide an important consideration in understanding and controlling the chemistry of other CVD processes since amido precursors are useful for the CVD of many nitride materials.[45] Currently we are exploring the generality of this effect for the gas-phase reactions of other metal amido complexes with $NH_3$ as well as the effect added amine has on the properties of TiN deposited.

**Acknowledgment.** This work was supported by Sematech and by The Aerospace Sponsored Research Program. Thanks are due Drs. B. Brady, R. Heidner, R. Martin, and M. Allendorf for critical comments.

JA953468O

(44) Preliminary data provide an estimate of the relative rate constants for $Ti(NMe_2)_4$ and $Ti(NEt_2)_4$ with $NH_3$ at 85 °C to be $k_{Me}/k_{Et} = 155$; Weiller, B. H. To be published.

(45) (a) Gordon, R. G.; Hoffman, D. M.; Riaz, U. *Mater. Res. Soc. Symp. Proc.* **1992**, *242*, 445−450. (b) Gordon, R. G.; Hoffman, D. M.; Riaz, U. *Chem. Mater.* **1992**, *4*, 68−71. (c) Gordon, R. G.; Riaz, U.; Hoffman, D. M. *J. Mater. Res.* **1992**, *7*, 1679−1684. (d) Hoffman, D. M. *Polyhedron* **1994**, *13*, 1169−1179.